

# What sets topographic relief in extensional footwalls?

Alexander L. Densmore\*

Department of Earth Sciences, ETH Zürich, CH-8092 Zürich, Switzerland

Nancye H. Dawers

Department of Earth and Environmental Sciences, Tulane University, New Orleans, Louisiana 70118, USA

Sanjeev Gupta

Department of Earth Science and Engineering, Imperial College, London SW7 2AZ, UK

Roman Guidon

Department of Earth Sciences, ETH Zürich, CH-8092 Zürich, Switzerland

## ABSTRACT

**We use three large normal fault arrays in the northeastern Basin and Range Province, western United States, to document catchment development and relief production during fault growth. Fault slip and slip rates increase systematically along strike from zero at the fault tips. Catchment relief and across-strike range width both increase as slip accumulates but reach maximum values at a distance of ~15 km from the fault tips and remain uniform along strike over much of the footwalls. Catchment outlet spacing also increases away from the fault tips but does not reach a uniform value and may vary by a factor of 5–6 along strike. We infer that catchments first elongate in the across-strike direction as slip accumulates and the range half-width increases. Once the half-width reaches its maximum value, continued catchment growth is possible only by along-strike capture, which increases outlet spacing but not relief. The close correspondence between catchment relief and range half-width suggests that geomorphically limited hillslope and channel gradients are achieved within the 15 km tip zone. Thus, the limiting factor in footwall development is the width of the range, which is controlled by two external agents: the geometry and spacing of the major faults, and the elevations of base level on both flanks.**

**Keywords:** normal faults, topography, tectonic geomorphology, landscape evolution, Idaho, Montana.

## INTRODUCTION

The geomorphic response of Earth's surface to lithospheric deformation is a fundamental research problem in studies of landscape evolution, but efforts to resolve it are commonly frustrated by our inability to characterize the three-dimensional deformation field that drives landscape development. One approach to this problem is to study the growth of simple discrete structures for which the deformation field can be readily defined. This permits direct and quantitative relation of topography to fault displacement, which is a crucial first step in understanding the topographic response to tectonics. However, measurement of the displacement field around growing structures is difficult over relevant time scales. Here we take advantage of the fact that faults show predictable along-strike variations in slip (Cowie and Scholz, 1992; Dawers et al., 1993; Bürgmann et al., 1994; Gupta and Scholz, 2000; Manighetti et al., 2001) and, moreover, slip rate (Cowie and Roberts, 2001; Roberts and Michetti, 2004). Because large faults propagate by interaction and linkage of segments (e.g., Cartwright et

al., 1995; Dawers and Anders, 1995; Dawers and Underhill, 2000; McLeod et al., 2000), fault tips undergo less slip and lower slip rates than the strike centers (e.g., McLeod et al., 2000; Cowie and Roberts, 2001).

In a previous paper (Densmore et al., 2004), we showed that footwall relief is nearly uniform along several large normal faults in the northeastern Basin and Range Province, western United States, and decays smoothly to zero at the fault tips over a distance of ~15 km. Densmore et al. (2004) hypothesized that this uniform relief is decoupled from the fault slip profile outside the 15 km tip zone. If most of the slip has accrued since linkage of these fault arrays, then we can examine the progressive development of the footwall using distance from the fault tip as a proxy for increasing slip rate (e.g., McLeod et al., 2000). In this paper we use observations of catchment morphology from three large footwall ranges to show how footwalls evolve in the face of increasing slip rate, and we argue that footwall relief is a simple function of fault geometry and spacing, modulated by base level and perhaps limited by geomorphic processes and rock mass strength.

## THROW PROFILES IN THE NORTHEASTERN BASIN AND RANGE

We focus on footwall topography developed on the normal-slip Beaverhead, Lemhi, and Lost River faults in the northeastern Basin and Range (Fig. 1A). All three faults are 140–150 km long and are composed of multiple linked segments. The faults appear to have largely reached their present extent by ca. 6 Ma (Anders et al., 1993; Anders, 1994; Anders and Schlische, 1994), so we are confident in using distance from the southeastern fault tips as a proxy for slip rate in examining catchment morphology and footwall evolution.

Along-strike variations in fault throw in the study area are relatively simple (Fig. 1B). Because we are interested in the geomorphic response to surface offset, we take the fault tips to coincide with the southeastern limits of the three footwall ranges (Fig. 1A). There is evidence for extensional fracturing in the Snake River Plain beyond the southeastern tip of the Lost River fault (Kuntz et al., 2002), but surface offsets are limited to a few meters and no similar structures are observed southeast of the Lemhi or Beaverhead faults. Throw data for the Beaverhead and Lemhi faults, although sparse, are remarkably consistent with the

\*E-mail: densmore@erdw.ethz.ch.

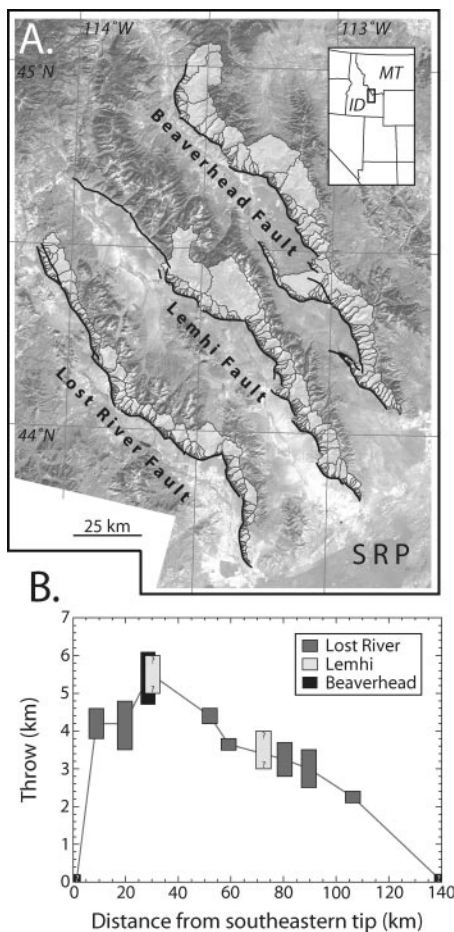


**Figure 1. A:** Map of study area in northeastern Basin and Range Province, western United States. Background is Landsat 7 image mosaic. SRP—Snake River Plain. Solid black lines show fault traces. **B:** Estimates of throw on Beaverhead, Lemhi, and Lost River faults as function of distance from southeastern fault tip. Fault tips are assumed to be at southeastern end of associated footwall topography. Height of each bar indicates range of throw estimates at that location, and width represents assumed error in along-strike position of  $\pm 2.5$  km. Estimates for Lost River fault are based on offset Paleozoic and Cenozoic strata and gravity data, and are taken from Janecke et al. (1991). Estimates for Beaverhead fault, and for Lemhi fault at  $x = 30$  km, are based on tilts of footwall volcanic rocks (Anders et al., 1993) plus assumed depths of basin fill (Rodgers and Anders, 1990; M. Anders, 2004, personal commun.). Estimate for Lemhi fault at  $x = 73$  km is based on tilts of Eocene Challis Formation volcanic rocks. Uncertainties in throw estimates are due to footwall erosion, lack of hanging-wall subsurface data (Anders et al., 1993), regional subsidence and volcanic activity (McQuarrie and Rodgers, 1998), and prior Cenozoic extension (e.g., Janecke et al., 2001).

better-constrained throw profile of the Lost River fault (Fig. 1B). Maximum throws are  $\sim 4$ – $6$  km, yielding a cumulative throw/length ratio for these faults of 0.03–0.04 (Densmore et al., 2004), very close to the global ratio of

$\sim 0.03$  of Schlische et al. (1996). The throw profiles are skewed toward the southeastern fault tips, with maximum values within 30–50 km of the tips. This skew could arise from variation in crustal properties (e.g., Bürgmann et al., 1994), subsidence of the Snake River Plain (McQuarrie and Rodgers, 1998), or from asymmetry in the long-term development of the faults (e.g., Manighetti et al., 2001). Older footwall topography and lithological contrasts inherited from earlier extensional episodes complicate the present landscape, particularly at the northwestern fault tips (e.g., Crone and Haller, 1991; Janecke et al., 2001). For simplicity, we focus on the southeastern 80 km of each footwall, where there is a clearly defined relationship between topography and the currently active faults.

### CATCHMENT GROWTH DURING SLIP ACCUMULATION

We measure basic catchment properties as a function of along-strike position, including relief from the fault to the drainage divide, range half-width, and outlet spacing. These measurements allow us to quantify along-strike changes in the shape of the catchments and the geometry of the footwall (see Data Repository<sup>1</sup>). We show results only from catchments that extend to the drainage divide, as these catchments define the topography of the entire footwall.

Catchment relief in all three footwalls increases monotonically from zero over the first  $\sim 15$  km from the fault tips (Densmore et al., 2004). This increase in footwall relief was interpreted by McQuarrie and Rodgers (1998) as due to subsidence of the Snake River Plain; however, similar patterns are observed in ranges that are not adjacent to the plain, including the Red Rock and Blacktail Ranges in Montana (Densmore et al., 2004). The increase in relief is mirrored by a smooth increase in the half-width of all three ranges over the same 15 km length scale (Figs. 2A–2C). Beyond this tip zone, both relief and half-width are relatively uniform for 65 km along strike and appear to covary with each other. The strong along-strike correlation between relief and half-width is reflected in the near-linear relationship for each footwall, which persists up to the maximum values of relief (Fig. 2D). Catchment outlet spacing is also low where relief is low, near the fault tips, and increases toward the strike centers. However, the increase is not limited to the same 15 km tip zone, and outlet spacing increases more slowly than half-width with increasing relief

(Fig. 2E). Because of this, outlet spacing is proportional to relief near the fault tips, but it can deviate from this relationship by as much as a factor of 5–6 at higher values of relief (Fig. 2E). Part of this variation is explained by footwall lithology; as noted by Densmore et al. (2004), the largest catchments in all three footwalls (Fig. 1A) are cut into sedimentary fills of older hanging-wall basins. However, this coincidence does not lead to increased footwall relief.

## DISCUSSION AND CONCLUSIONS

### Implications for Catchment Growth

Because range half-width and outlet spacing are measures of catchment size in the across-strike and along-strike directions, respectively, their relationships show how catchments grow with increasing fault slip. We infer a two-stage process of catchment growth in the study area (Fig. 3). In the first stage, half-width and outlet spacing both increase with increasing footwall relief. However, because half-width increases more rapidly than outlet spacing (Figs. 2D, 2E), initial catchment growth is primarily by elongation in the across-strike direction (Fig. 3A).

The first stage persists until footwall relief reaches its maximum value of 1000–1500 m, which occurs  $\sim 15$  km from the fault tip (Densmore et al., 2004) and corresponds to a transition to uniform half-width (Fig. 2A). In the second stage of catchment growth, the relatively invariant half-width means that any further enlargement must occur by along-strike drainage reorganization and drainage area competition (e.g., Ellis et al., 1999). This results in increased catchment area and thus outlet spacing, but no change in relief or half-width (Fig. 2D).

Thus, catchment growth does not appear to be a self-similar process, in the sense that a constant aspect ratio of catchment length to width is not maintained during slip accumulation. Instead, catchment growth is dominated first by elongation in the across-strike direction, followed by widening in the along-strike direction (Fig. 3). Frankel and Pazzaglia (2005) inferred a similar evolutionary history for footwall catchments on the basis of ratios of catchment volume to area.

### External Controls on Range Width and Relief

Why is relief so uniform along strike in these footwalls? The southern limit of valley glaciation in all three ranges is to the north of the 15 km tip zone, so glacial erosion is unlikely to be the cause of limited relief (e.g., Brocklehurst and Whipple, 2002). The spatial correlation between catchment relief and range half-width (Figs. 2A–2C) shows that relief and half-width are inextricably linked during the evolution of footwall topography in

<sup>1</sup>GSA Data Repository item 2005085, Measurement of footwall catchment morphology, is available online at [www.geosociety.org/pubs/ft2005.htm](http://www.geosociety.org/pubs/ft2005.htm), or on request from [editing@geosociety.org](mailto:editing@geosociety.org) or Documents Secretary, GSA, P.O. Box 9140, Boulder, CO 80301-9140, USA.

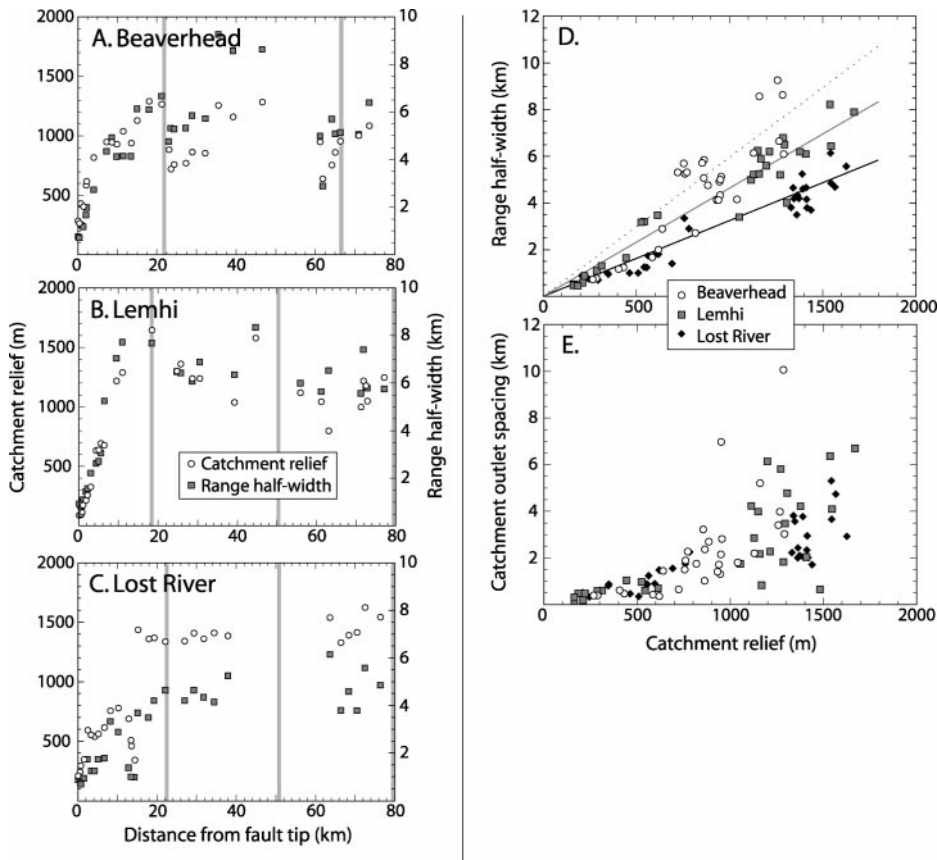


**Figure 2.** A–C: Along-strike profiles of catchment relief (circles) and range half-width (squares) as functions of distance from southeastern fault tips for three footwalls in study area. Only catchments that define drainage divide are shown. Note uniform width and relief values beyond ~15 km from fault tips. Gray bars show boundaries between fault segments. D: Relationship between catchment relief and range half-width for all three footwalls. Lines show least-square regression through data for each footwall. Note linear relationship up to and including largest values of relief. E: Relationship between relief and catchment outlet spacing. Outlet spacing increases only slowly with increasing relief and is variable even at highest values of relief.

the study area. The simplest explanation is that footwall relief is a geometric consequence of the available space within the footwall, which is controlled by the half-width. Any increase in relief requires a concomitant increase in half-width. This depends critically on the establishment, within the 15 km tip zone, of hillslope and channel gradients that are geomorphically limited by the conspiracy of rock-mass strength and local climate. If this were not true, footwall relief could continue to grow beyond the 15 km tip zone—even with fixed width—through steepening of hillslopes and channels. Because relief stops increasing at the same point that half-width stops increasing, gradients in the catchments must have already achieved maximum values (Densmore et al., 2004). This could occur through a transition to more efficient erosional processes, such as bedrock landsliding (Burbank et al., 1996) and debris flows, driven by higher slip rates away from the fault tip. The occurrence of such a process transition within the 15 km tip zone is a testable prediction of our model.

What determines the range width? We sug-

gest two primary controls (Fig. 4): the width of the tectonic topography created by fault slip, and the position of base level on either side of the range. The width of the tectonic topography is determined by the geometry and spacing of the faults. Observations and elastic models of coseismic slip on the Lost River fault show that the width of the uplifting footwall is a function of fault dip and thickness of the seismogenic layer (Fig. 4A; Stein and Barrientos, 1985). Faults with closely spaced neighbors, such as the Lemhi fault, have even narrower tectonic topographies than isolated faults because of interference between the displacement fields (Anders et al., 1993); this represents an extra constraint on the space available for footwall topography.

In turn, the width of the tectonic topography may not match the width of the resulting range because of the influence of base level on both flanks of the footwall (Fig. 4B). The widths will be equal only if the pre-faulting surface is horizontal and is maintained as regional base level on both flanks of the range. If base level is raised, then the resulting deposition will

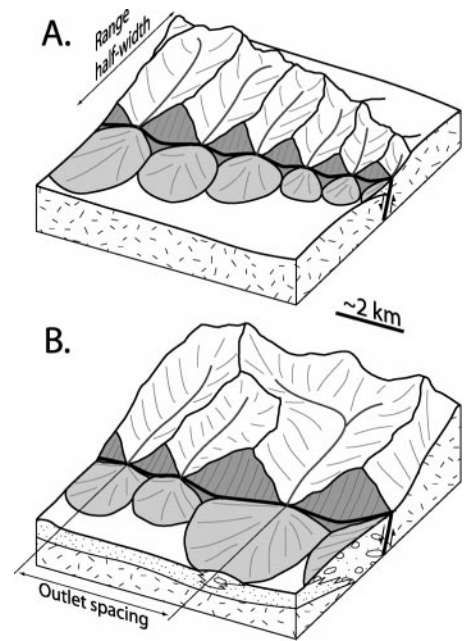


**Figure 3.** Schematic view of catchment growth at two different stages in evolution of footwall. A: Early stage, with low slip and slip rate. Catchments grow by headward elongation in across-strike direction, which increases relief and range half-width. Outlet spacing increases only slowly. B: Later stage, by which time relief and half-width have reached uniform values. Additional catchment growth is only possible by widening in along-strike direction, which increases outlet spacing but does not affect relief.

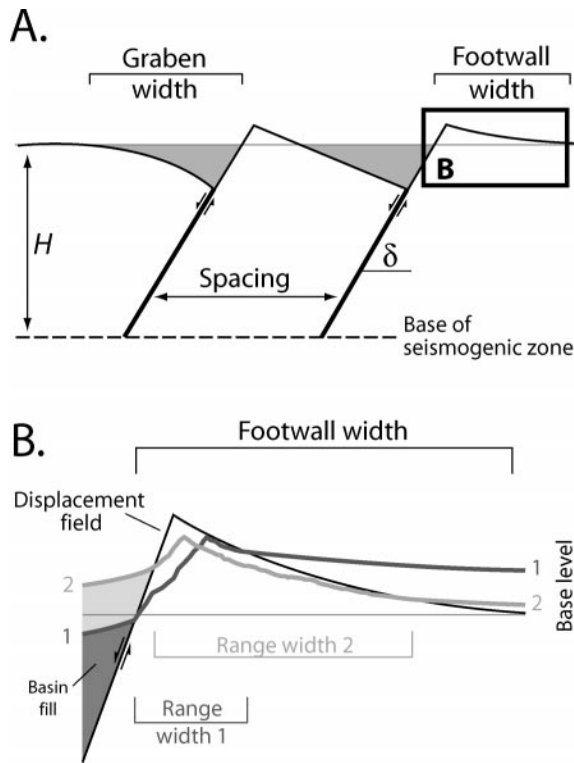
bury part of the tectonic topography, leading to a decrease in range width. Variations in base level on the rear flank of the footwall, opposite the fault, will be particularly effective at changing range width because of the low gradient in the displacement field (Fig. 4B). Because base level is in part determined by sediment supply from the footwall, there are complex links between slip accumulation, erosion and mass transfer, base-level change, and footwall relief.

We propose a model of footwall evolution in the study area in which the width of the range grows with increasing fault slip and slip rate until it is limited by fault spacing and base level in adjacent basins. Footwall relief increases as the range gets wider, but once the range width is limited, relief can no longer continue to increase, perhaps because of geomorphically limited gradients. Beyond this point, footwall morphology is decoupled from along-strike variations in slip rate. Thus, both mountain range width and relief are controlled by the geometry and spacing of the faults, overprinted by the effects of base level in adjacent basins.

#### ACKNOWLEDGMENTS

This research was supported by grants from the U.S. National Science Foundation (EAR-0207569)

**Figure 4. Controls on range width. A: Tectonic controls on width of footwall tectonic topography. Footwall width is proportional to fault dip  $\delta$  and thickness of seismogenic layer  $H$  (Scholz and Contreras, 1998). Shaded areas show regions of hanging-wall subsidence. If fault spacing is small, this will limit footwall width to less than expected value because of domino-like interference between adjacent fault blocks (e.g., Anders et al., 1993). B: Effects of base level on range width. Tectonic topography (thin black line) is modified by height of base level on both sides of range. Two examples are shown. In first (dark gray), base level is low in hanging wall and high on back side of footwall, leading to very narrow range. In second, base level is higher in hanging wall and lower on back side, yielding wider range whose width approaches that of tectonic topography.**



and the Swiss National Science Foundation (2100-067624). Michael Ellis wrote or inspired many of the Matlab routines used to analyze footwall topography. Mark Anders and Susanne Janecke provided useful advice on constraining the fault throw profiles. We thank Guy Simpson, Ralf Hetzel, Brian McAdoo, Michael Ellis, Kurt Frankel, Philip Allen, and Colin Stark for helpful discussions. Joe Cartwright, George Hille, and David Rodgers provided excellent and constructive reviews.

#### REFERENCES CITED

Anders, M.H., 1994, Constraints on North American plate velocity from the Yellowstone hot-spot deformation field: *Nature*, v. 369, p. 53–55.

Anders, M.H., and Schlische, R.W., 1994, Overlapping faults, intrabasin highs, and the growth of normal faults: *Journal of Geology*, v. 102, p. 165–180.

Anders, M.H., Spiegelman, M., Rodgers, D.W., and Hagstrum, J.T., 1993, The growth of fault-bounded tilt blocks: *Tectonics*, v. 12, p. 1451–1459.

Brocklehurst, S.H., and Whipple, K.X., 2002, Glacial erosion and relief production in the Eastern Sierra Nevada, California: *Geomorphology*, v. 42, p. 1–24.

Burbank, D.W., Leland, J., Fielding, E., Anderson, R.S., Brozovic, N., Reid, M.R., and Duncan, C., 1996, Bedrock incision, rock uplift and threshold hillslopes in the northwestern Himalayas: *Nature*, v. 379, p. 505–510.

Bürgmann, R., Pollard, D.D., and Martel, S.J., 1994, Slip distributions on faults: Effects of stress gradients, inelastic deformation, heterogeneous host-rock stiffness, and fault interaction: *Journal of Structural Geology*, v. 16, p. 1675–1690.

Cartwright, J.A., Trudgill, B.D., and Mansfield, C.S., 1995, Fault growth by segment linkage: An explanation for scatter in maximum dis-

placement and trace length data from the Canyonlands Graben of SE Utah: *Journal of Structural Geology*, v. 17, p. 1319–1326.

Cowie, P.A., and Roberts, G.P., 2001, Constraining slip rates and spacings for active normal faults: *Journal of Structural Geology*, v. 23, p. 1901–1915.

Cowie, P.A., and Scholz, C.H., 1992, Displacement-length scaling relationship for faults: Data synthesis and discussion: *Journal of Structural Geology*, v. 14, p. 1149–1156.

Crone, A.J., and Haller, K.M., 1991, Segmentation and coseismic behavior of Basin and Range normal faults: Examples from east-central Idaho and southwestern Montana: *Journal of Structural Geology*, v. 13, p. 151–164.

Dawers, N.H., and Anders, M.H., 1995, Displacement-length scaling and fault linkage: *Journal of Structural Geology*, v. 17, p. 607–614.

Dawers, N.H., and Underhill, J.R., 2000, The role of fault interaction and linkage in controlling synrift stratigraphic sequences: Late Jurassic, Statfjord East area, northern North Sea: *American Association of Petroleum Geologists Bulletin*, v. 84, p. 45–64.

Dawers, N.H., Anders, M.H., and Scholz, C.H., 1993, Growth of normal faults: Displacement-length scaling: *Geology*, v. 21, p. 1107–1110.

Densmore, A.L., Dawers, N.H., Gupta, S., Guidon, R., and Goldin, T., 2004, Footwall topographic development during continental extension: *Journal of Geophysical Research*, v. 109, doi: 10.1029/2003JF000115.

Ellis, M.A., Densmore, A.L., and Anderson, R.S., 1999, Development of mountainous topography in the Basin Ranges, USA: *Basin Research*, v. 11, p. 21–41.

Frankel, K., and Pazzaglia, F.H., 2005, Mountain fronts, base level fall, and landscape evolution: Insights from the southern Rocky Mountains, *in* Willett, S., et al., eds., *Tectonics, cli-*

mate, and landscape evolution: Geological Society of America Special Paper (in press).

Gupta, A., and Scholz, C.H., 2000, A model of normal fault interaction based on observations and theory: *Journal of Structural Geology*, v. 22, p. 865–879.

Janecke, S.U., Geissman, J.W., and Bruhn, R.L., 1991, Localized rotation during Paleogene extension in east central Idaho: Paleomagnetic and geologic evidence: *Tectonics*, v. 10, p. 403–432.

Janecke, S.U., Blankenau, J.J., VanDenburg, C.J., and Van Gosen, B.S., 2001, Map of normal faults and extensional folds in the Tendency Mountains and Beaverhead Range, southwest Montana and eastern Idaho: U.S. Geological Survey Miscellaneous Field Studies Map MF-2362, scale 1:100,000.

Kuntz, M.A., Anderson, S.R., Champion, D.E., Lanphere, M.A., and Grunwald, D.J., 2002, Tension cracks, eruptive fissures, dikes, and faults related to late Pleistocene–Holocene basaltic volcanism and implications for the distribution of hydraulic conductivity in the eastern Snake River Plain, Idaho, *in* Link, P.K., and Mink, L.L., eds., *Geology, hydrogeology, and environmental remediation: Idaho National Engineering and Environmental Laboratory, eastern Snake River Plain, Idaho: Geological Society of America Special Paper 353*, p. 111–133.

Manighetti, I., King, G.C.P., Gaudemer, Y., Scholz, C.H., and Doubre, C., 2001, Slip accumulation and lateral propagation of active normal faults in Afar: *Journal of Geophysical Research*, v. 106, p. 13,667–13,696.

McLeod, A.E., Dawers, N.H., and Underhill, J.R., 2000, The propagation and linkage of normal faults: Insights from the Strathspey–Brent–Statfjord fault array, northern North Sea: *Basin Research*, v. 12, p. 263–284.

McQuarrie, N., and Rodgers, D.W., 1998, Subsidence of a volcanic basin by flexure and lower crustal flow: The eastern Snake River Plain, Idaho: *Tectonics*, v. 17, p. 203–220.

Roberts, G.P., and Michetti, A.M., 2004, Spatial and temporal variations in growth rates along active normal fault systems: An example from the Lazio–Abruzzo Apennines, central Italy: *Journal of Structural Geology*, v. 26, p. 339–376.

Rodgers, D.W., and Anders, M.H., 1990, Neogene evolution of Birch Creek Valley near Lone Pine, Idaho, *in* Roberts, S., ed., *Geologic field tours of western Wyoming and parts of adjacent Idaho, Montana, and Utah: Geological Survey of Wyoming Public Information Circular 29*, p. 27–38.

Schlische, R.W., Young, S.S., Ackermann, R.V., and Gupta, A., 1996, Geometry and scaling relations of a population of very small rift-related normal faults: *Geology*, v. 24, p. 683–686.

Scholz, C.H., and Contreras, J.C., 1998, Mechanics of continental rift architecture: *Geology*, v. 26, p. 967–970.

Stein, R.S., and Barrientos, S.E., 1985, Planar high-angle faulting in the Basin and Range: Geodetic analysis of the 1983 Borah Peak, Idaho, earthquake: *Journal of Geophysical Research*, v. 90, p. 11,355–11,366.

Manuscript received 6 December 2004  
 Revised manuscript received 25 February 2005  
 Manuscript accepted 28 February 2005

Printed in USA